Weak Dependence of Mobility of Membrane Protein Aggregates on Aggregate Size Supports a Viscous Model of Retardation of Diffusion

Dennis F. Kucik,* Elliot L. Elson,[#] and Michael P. Sheetz[§]

*Department of Pathology, University of Alabama, Birmingham, Birmingham, Alabama 35294; [#]Department of Biochemistry and Molecular Biophysics, Washington University School of Medicine, St. Louis, Missouri 63110; and [§]Department of Cell Biology, Duke University Medical Center, Durham, North Carolina 27110 USA

ABSTRACT   Proteins in plasma membranes diffuse more slowly than proteins inserted into artificial lipid bilayers. On a long-range scale (>250 nm), submembrane barriers, or skeleton fences that hinder long-range diffusion and create confinement zones, have been described. Even within such confinement zones, however, diffusion of proteins is much slower than predicted by the viscosity of the lipid. The cause of this slowing of diffusion on the micro scale has not been determined and is the focus of this paper. One way to approach this question is to determine the dependence of particle motion on particle size. Some current models predict that the diffusion coefficient of a membrane protein aggregate will depend strongly on its size, while others do not. We have measured the diffusion coefficients of membrane glycoprotein aggregates linked together by concanavalin A molecules bound to beads of various sizes, and also the diffusion coefficients of individual concanavalin A binding proteins. The measurements demonstrate at most a weak dependence of diffusion coefficient on aggregate size. This finding supports retardation by viscous effects, and is not consistent with models involving direct interaction of diffusing proteins with cytoskeletal elements.

INTRODUCTION

Proteins in cell membranes typically diffuse much more slowly than do proteins in artificial lipid bilayers. Although the simplest hydrodynamic theory predicts that lateral diffusion of proteins in cell membranes should be roughly half as fast as that of lipids (Saffman and Delbruck, 1975), the experimentally measured ratio is often one to three orders of magnitude (Jacobson et al., 1987). Both long-range and short-range protein diffusion is slower than expected from interaction with lipids.

Much has been learned recently about retardation of long-range diffusion. It is clear that in many cells, long-range diffusion is restricted by confinement zones of 250-1500-nm diameter. In such zones, proteins reside from ~3–35 s before they move to the next confinement zone (Saxton and Jacobson, 1997). This has been attributed to encounters with a "membrane skeleton fence" in fibroblasts (Sako and Kusumi, 1995). Within each confinement zone, diffusion is relatively fast, but long-range diffusion is slowed by barriers between compartments.

Even "fast" diffusion of proteins within such compartments, however, is much slower than in pure lipid bilayers. Therefore, factors not readily apparent by simple single particle tracking (SPT) measurements operate to retard dif-

fusion on the micro scale, independent of the barriers that have been described. This freer, but still retarded, diffusion within compartments is characterized by D_{micro}, the diffusion coefficient within a compartment, determined from the initial slope of the mean-square displacement plot versus the time interval (Sako and Kusumi, 1995).

The three basic models of retardation of diffusion, as we envision them, are depicted in Fig. 1. The first involves *obstruction* by *membrane microcorrals* (Fig. 1 *A*). This model proposes that within confinement zones there exist a similar set of weaker barriers, too small to be detected directly on the time scale of SPT. These would behave much like the larger confinement zones, slowing diffusion over distances greater than the span of the microcorral. These microcorrals would have to be <~0.1 μm across, however, since they are not readily detectable by examination of SPT particle tracks. Direct evidence for interactions of membrane proteins with corrals of this size is lacking. It has been suggested, however, that obstruction by such barriers may account for the gap between hydrodynamic theory and experimental measurement in some systems (Bussell et al., 1995a; Dodd et al., 1995).

While identification of the specific proteins comprising these barriers to diffusion is beyond the scope of this study, we suggest that a candidate protein would be actin itself. Electron micrographs of the lamella of the fish epidermal keratocyte show that the actin cytoskeleton underlying the plasma membrane in the lamella forms a tight meshwork, the size of which is consistent with microcorrals (Svitkina et al., 1997). Such an actin network configuration is also typical of many fibroblastic cells.

The second model involves rapid and repetitive *transient binding* to and release from slowly moving or immobile structures, on a time scale so fast that individual binding
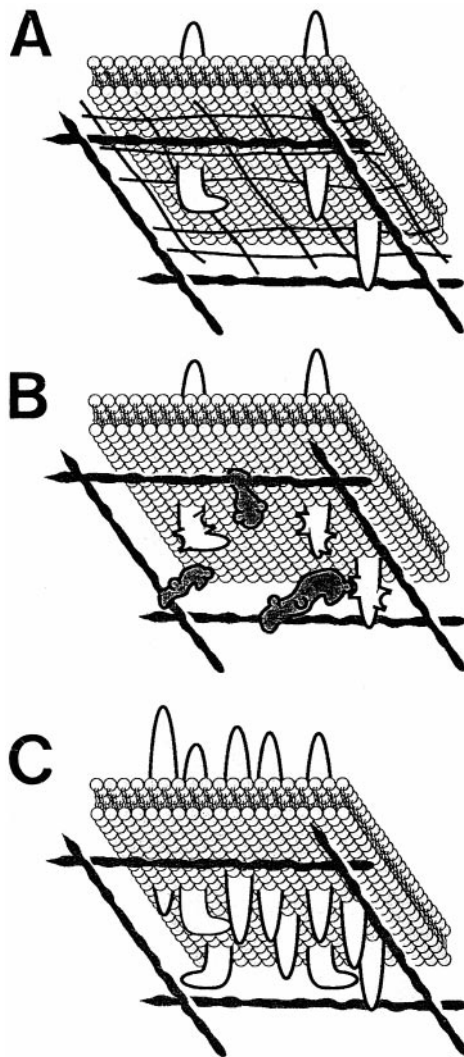

FIGURE 1 Models of retardation of diffusion on the micro scale. (*A*) The microcorral model. This model proposes that within confinement zones there exists a similar set of weaker barriers, too small to be detected directly on the time scale of SPT. These barriers retard membrane protein diffusion over distances greater than the span of the microcorral. Because of their small size ($<\sim$0.1 μm across), these microcorrals would not be detectable by examining SPT particle tracks. (*B*) The transient binding model. This model predicts that the diffusion of cell surface proteins is impeded by interactions between the mobile proteins and slowly moving or immobile structures in the cytoplasm, e.g., cytoplasmic proteins bound to the cytoskeleton (cf Zhang et al., 1991). The example illustrated depicts an indirect interaction with the cytoskeleton via a single cytoplasmic protein; a variety of other indirect links would have the same effect. If the lifetime of the bound state were short compared to the measurement time, the diffusion coefficient would be reduced by the fraction of the time it spent in the bound state (Elson and Reidler, 1979). (*C*) A viscous model. This illustration depicts protein crowding as the source of high apparent viscosity. Alternatively, high apparent viscosity might be due to other sources of drag, such as viscous interactions with intra- or extracellular structures (Zhang et al., 1991), excluded area effects (Saxton, 1990), or hydrodynamic effects of immobile proteins (Bussell et al., 1995b).

events would not be discernible by SPT measurements (Fig. 1 *B*). Although this is not a new idea, recent support for this model comes from experiments with band 3, the major membrane protein of the erythrocyte (Golan et al., 1996). In that system, both lateral and rotational mobility of band 3 was higher in erythrocytes deficient in the protein band 4.2 than in normal cells. Since band 4.2 binds both band 3 and elements of the cortical cytoskeleton, a plausible explanation for this retardation of diffusion would be that transient binding to the cytoskeleton, via band 4.2, retards both rotational and lateral motion of band 3. As pointed out by Bussell et al. (1995a), not all of the retardation of band 3 can be explained by current hydrodynamic theory. The typical nucleated cell, however, is very different from the erythrocyte with a much less structured cytoskeleton underlying the plasma membrane. Strong evidence for or against transient binding to explain retardation of diffusion in nucleated cells is, to our knowledge, currently lacking.

Finally, simple *viscous resistance* to membrane protein motion might slow diffusion on the micro scale. This viscous resistance, however, would have to be much greater than that expected from the lipids of the membrane bilayer itself. One likely source of this increased apparent viscosity is the effect of other membrane proteins, especially immobile ones (Fig. 1 *C*). Relatively few immobile proteins can have profound effects on the effective viscosity of the plasma membrane. In this model, the diffusion of a "tracer" protein is slowed by the effect of other proteins embedded in the same lipid bilayer. This represents the current state of the hydrodynamic model (discussed in more detail in the Discussion section) (Bussell et al., 1995a, c; Dodd et al., 1995). It is important to note, however, that our study does not distinguish among possible sources of increased viscosity. Therefore, this model is meant to encompass increased viscosity due to any source, including protein crowding (excluded area effects) (Saxton, 1990), hydrodynamic effects of mobile or immobile proteins (Bussell et al., 1995a, c; Dodd et al., 1995), viscous interactions with the cytoplasm or with the glycocalyx coating the cell's outer surface (Zhang et al., 1991), or a combination of all of these.

While all three models predict similar behavior for individual membrane proteins, they differ in their predictions for the rate of lateral diffusion of membrane proteins clustered in aggregates of various sizes. In particular, the first two, which involve direct interaction with the cytoskeleton, predict a strong dependence on aggregate size, while the last, which involves only viscous interactions, does not. We formed membrane protein aggregates by coating beads (ranging in diameter from 40 to 550 nm) with con A and allowing them to attach to membrane proteins on the cell surface. Theory predicts that the region of contact between a bead and the cell surface should increase with the size of the bead (see Discussion section and Appendix). The number of glycoproteins bound should also increase with the contact area, a consideration important for evaluating the transient binding and model. By using this approach we have been able to discriminate among models.

To measure diffusion rates, we used FRAP for individual proteins (Axelrod et al., 1976), and used SPT (Sheetz et al., 1989; Qian et al., 1991; de Brabander et al., 1991) for

bead-induced aggregates. SPT uses small ligand-coated gold or latex beads to tag membrane proteins. Larger beads form aggregates by accumulating a number of protein molecules proportional to the area of contact between the bead and the cell membrane. These are then tracked with high resolution using video-enhanced DIC microscopy. Random and directed components of motion can be separated unambiguously (Sheetz et al., 1989; for a detailed discussion of theory, see Qian et al., 1991) and movement of the cell can be subtracted (Kucik et al., 1990). We used con A, a lectin that binds many species of membrane glycoproteins, to coat the beads. Thus, the behavior of the beads should reflect a general property of membrane proteins, rather than interactions specific to a particular membrane protein.

We made these measurements on fish epidermal keratocytes (FEKs) because of their favorable optical properties and the relative lack of surface features, such as ruffles, which might influence diffusion (Kucik et al., 1990). Also, in many cell types, large con A-coated beads often induce nondiffusional behavior, e.g., rearward transport, perhaps due to cross-linking of certain receptors (unpublished observations). In FEKs, however, although a few beads undergo directed transport, the vast majority (>95%) of con A-coated beads of all sizes display only diffusional behavior for several minutes (Kucik et al., 1991).

We measured the diffusion coefficients of membrane proteins by both FRAP and SPT in the same system, FEKs, with the same membrane protein ligand, con A, always at room temperature (a physiologic temperature for goldfish). Because we could not directly measure the area of contact between the beads and the cell membrane, we used a model calculation to predict how the size of the aggregate should vary with the bead diameter (see Appendix). As previously observed on FEKs and other cell types, the measured rates of diffusion (D_{micro}) for the smallest beads were orders of magnitude slower than theoretically expected for ideal diffusion in a pure lipid bilayer, but well within the range of actual FRAP measurements of diffusion coefficients of individual membrane proteins on a variety of living cells (Jacobson et al., 1987). This suggests that the same factors that slow protein movement on more commonly studied cells also operate in the FEK cell system, making it a valid system to study.

The dependence of diffusion on aggregate size was found to be very weak. Equally striking, diffusion coefficients of beads measured by SPT do not differ substantially from those of individual glycoproteins labeled with fluorescein-labeled succinyl con A and measured by FRAP. These observations are inconsistent with "transient binding" and "microcorral" models, but favor a hydrodynamic model, i.e., that the membrane proteins move as if embedded in a very viscous two-dimensional fluid (discussed below).

MATERIALS AND METHODS

Cells

Scales were removed from goldfish (*Carassius auratus*), and placed on acid washed glass coverslips in the presence of bovine serum (Kolega,

1986). FEK cells that crawled onto the glass were then cultured in fish Ringer's supplemented with Amphibian medium obtained from Gibco (Life Technologies, Inc., Gaithersburg, MD) as described in Cooper and Schliwa (1986). The coverslips were then transferred to a stage medium of fish Ringer's for microscopy.

Single particle tracking

Latex beads (Polysciences, Inc. Warrington, PA) and gold beads (Janssen Pharmaceuticals, Piscataway, NJ) were coated with con A by adsorption as described earlier (Sheetz et al., 1989). These were added to the cells in a Ringer's solution stage medium, their motions were observed by video-enhanced differential interference contrast microscopy, and images were recorded on sVHS videotape for later analysis. Bead positions in each frame were determined by computer by the method of Gelles et al. (1988). From these position measurements diffusion coefficients were determined as described in Results and Discussion.

Con A-coated colloidal gold particles (40-nm diameter) and latex beads (190- and 550-nm diameter) bound to the cell surface via membrane glycoproteins. Beads were allowed to bind passively (40-nm gold) or were placed on the cell with laser tweezers. This binding was specific: it could be blocked by incubating the con A-coated particles with glycoproteins before an experiment (data not shown). Whether the particle was diffusing freely in the membrane or was anchored to the cytoskeleton was determined unambiguously from the diffusion coefficient of each bead as previously described (Sheetz et al., 1989; Kucik et al., 1989). Briefly, diffusion coefficients of diffusing beads are orders of magnitude greater than those of beads anchored via membrane proteins to the cytoskeleton (Sheetz et al., 1989; Kucik et al., 1990). Nearly all beads (>95%) diffused randomly, except for those very near the edge of the cell or a few that underwent cytoskeleton-driven rearward transport. The motion of these atypical beads was not analyzed.

The SPT measurements were performed on both locomoting and stationary cells. On locomoting cells diffusing particles move passively along with the cell, as described earlier (Kucik et al., 1990): in the frame of reference of the cell the particle motion is completely random. Brownian motion of the particle was analyzed independently of the directed motion component (Qian et al., 1991); see also Results section and Fig. 2.

Fluorescence photobleaching

FITC-s-con A was obtained from Sigma Chemical Co., St. Louis, MO. Fluorescence photobleaching measurements of labeled proteins in keratocyte membranes labeled with FITC-s-con A were carried out as previously described (Dubinsky et al., 1989).

Because we are assuming purely random motion of fluorophores (Axelrod et al., 1976), directed motion of unbleached fluorophores into the bleached spot can yield an artefactually elevated diffusion coefficient (*D*). Therefore, we were careful to eliminate any component of directed motion of the fluorophore. Apparent directed motion can result from drift of the microscope stage, cell migration, or systematic transport of cell surface features or particles. Systematic drift of the microscope stage relative to the laser beam was ruled out by occasionally bleaching a spot in the FITC-s-con A adsorbed to the glass coverslip in regions devoid of cells. The immobilized fluorophores indicated that drift of the microscope stage relative to the laser beam was undetectable in our measurements. Distortion of the FRAP measurements by active motions of normal cells was suppressed by treating the cells with 10 mM $CoCl_2$ or cytochalasin D (2 μg/ml). Cobalt ion frequently paralyzes the cells without altering their morphology or their actin cytoskeleton (Cooper and Schliwa, 1986). Although cytochalasin D caused most cells to retract their lamellae, there were enough cells which remained both spread and immobile so that diffusion measurements could be carried out. All diffusion measurements were made on the lamellar portion of the cell.

It has become clear in recent years that many membrane proteins are neither randomly diffusing nor immobile, but are undergoing systematic

FIGURE 2 Examples of data produced by the SPT method and their analysis. Panels (*A*) and (*B*) are examples of particle tracks of 40-nm gold and 550-nm latex beads, respectively. Particle tracks yielding diffusion coefficients near the mean for each group were chosen for this example. In this case, each particle track is 363 points in length, each point representing a particle position measurement. Measurements were taken every 1/30 s, i.e., video frame rate. Bar = 1 μm. Mean length of particle tracks analyzed was 608 points = 20 s. Panels (*C*) and (*D*) are plots of msd of the particles in (*A*) and (*B*), respectively. For a particle diffusing in two dimensions, msd = 4*Dt*, where *D* is the diffusion coefficient. The displacement *d* of a particle undergoing directed motion at constant velocity *V* is described by $d = Vt$ and msd = $(Vt)^2$. Hence the random and directed components of particle motion can be extracted by fitting the msd to the equation msd = $4Dt + (Vt)^2$, and the diffusion coefficient can be determined [for a complete discussion of this analysis, see Qian et al. (1991)].
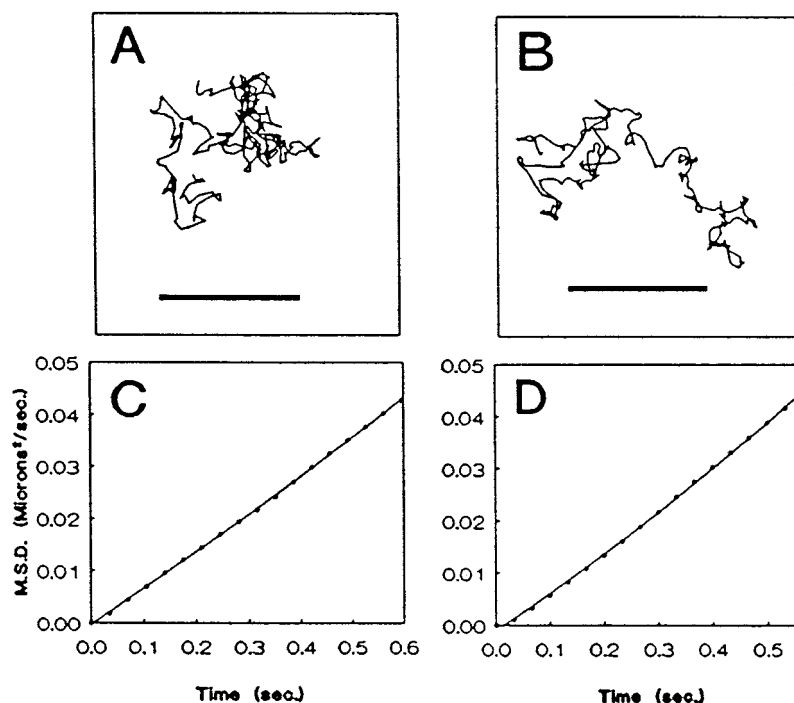
transport. Contributions of systematic fluorophore transport to fluorescence recovery can be assessed by varying the magnification of the objective lens, and therefore the size of the bleached spot. For simple diffusion the characteristic time for fluorescence recovery, τ_D, varies as the square of the radius of the photobleached spot, w, i.e., $\tau_D = w^2/4D$, where D is the diffusion coefficient (Axelrod et al., 1976). Contributions from transport mechanisms other than random diffusion cause the characteristic recovery time to vary from a simple dependence on w^2. Although most of our measurements were made with a 100× objective ($w = 2.1$ μm), the 40× ($w = 0.84$ μm) was occasionally used to rule out nonrandom motion of fluorophores. Comparison of measurements made with the two objectives often detected nonrandom motion in unparalyzed cells, usually due to movement of the cell itself. After the cells were paralyzed by $CoCl_2$ or cytochalasin D, however, systematic drift was never detected by this method. In addition, each cell was carefully observed before and after FRAP measurements to control for motion of the cell or its surface features.

Electron microscopy

Shortly after the addition of 0.5-μm con A beads, the cells were fixed according to a procedure described previously (Martenson et al., 1993). Fixative was added while the sample was being viewed by video-enhanced DIC microscopy to determine that cell morphology was not altered by fixative. After fixation and embedding, the glass microscope slide was removed and the specimen embedded in epon was examined to identify the regions of interest. Those regions were cut out and re-embedded in epon for sectioning with an orientation such that ultrathin sections were cut perpendicular to the original glass surface with a diamond knife. Sections were viewed on a Phillips 301 microscope.

RESULTS AND DISCUSSION

Sixty-six beads were tracked by SPT on 12 different days. In each experiment, beads of a particular size were added to a cell chamber, and motion was observed with video-enhanced DIC and recorded onto sVHS videotape. Fig. 2, *A* and *B* are examples of particle tracks generated by a 40-nm

con A-coated gold bead and a 550-nm con A-coated latex bead. Such particle tracks result from frame-by-frame analysis of video sequences, with particle positions accurately determined by the method of Gelles et al. (1988). Plots of mean square displacement versus time were generated from these particle tracks (Fig. 2, *C* and *D*). Under our experimental conditions, >95% of beads of all sizes diffused freely. Those that did not usually were only transiently immobilized. Particle tracks were analyzed, and diffusion coefficients (*D*) were calculated for those whose motion was random (not directed or restricted in the frame of reference of the cell).

While movement of the cell during the time course of the measurement contributed a directed component to the particle track (in the frame of reference of the lab), SPT measurements permit the separation of the random and systematic contributions to the motion of an individual bead, as previously explained (Sheetz et al., 1989; Qian et al., 1991). Briefly, purely random motion results in a linear increase in msd with elapsed time, *t*, i.e.,

$$msd_{random} = 4Dt \qquad (1)$$

For a constant velocity component of directed motion (such as that contributed by movement of the cell), $d = Vt$ and

$$msd_{directed} = (Vt)^2 \qquad (2)$$

where d = displacement and V = velocity. Thus, for a diffusing particle on the surface of a cell moving at constant velocity,

$$msd_{total} = 4Dt + (Vt)^2. \qquad (3)$$

By fitting this quadratic equation to the data, the random diffusion component of motion can be separated from the

directed movement of the cell, and a diffusion coefficient can be determined (Qian et al., 1991; Kucik et al., 1989). Fig. 3 summarizes the results of this analysis of 66 diffusing particles. The mean D values of the smallest and the largest particles differ by less than a factor of 2.

Diffusion coefficients obtained by SPT were compared to those obtained by photobleaching FITC s-con A-labeled membrane proteins. Like con A, s-con A labels a variety of membrane proteins, but is thought to cause less cross-linking due to its lower valency. Thus we could examine the behavior of individual membrane proteins or, at the most, small oligomers. Since FEKs are rapidly motile cells and fluorescence photobleaching is not as well suited as SPT to separating random motion of membrane proteins from directed motion of the cell, it was necessary to paralyze the cells to prevent movement of the bleached spot on the time scale of the measurements. We did this with cytochalasin D (2 μg/ml), which disrupts actin filaments (sometimes causing cells to round up; measurements were made only on cells which retained flat lamellae), and in separate experiments with $CoCl_2$, which paralyzes FEKs without greatly altering their morphology or disrupting the actin cytoskeleton (Cooper and Schliwa, 1986).

A total of 14 measurements were made on cytochalasin D-treated cells, and 50 measurements on $CoCl_2$-treated cells. The diffusion coefficient of s-con A on FEK calculated from these measurements was 8.6 $\pm$ 4.6 $\times$ 10^{-10} cm²/s for $CoCl_2$-treated cells, and 7.2 $\pm$ 2.8 $\times$ 10^{-10} cm²/s for cytochalasin D-treated cells (Fig. 4). The data obtained

FIGURE 4   Distribution of diffusion coefficients obtained from fluorescence photobleaching data. Membrane proteins were labeled with FITC-s-con A and their diffusion coefficients were measured by bleaching a spot and monitoring the time course of recovery of fluorescence. Since FEKs are highly motile cells, all cells were paralyzed for these experiments so that the bleached spot would not move during the measurement due to cell movement. Both cytochalasin D and cobalt chloride (cf. Cooper and Schliwa, 1986; also see text) were used to paralyze cells. The magnitudes and distribution of the diffusion coefficients agree well with typical values for membrane proteins on many types of cells (Jacobson et al., 1987).

with the two methods of paralyzing cell movement are in good agreement with each other. These values are also well within the range of diffusion coefficients measured FRAP for many different membrane proteins on a variety of other cells (Jacobson et al., 1987). Data from all FRAP and SPT measurements are summarized in Table 1.

Our major experimental result, therefore, is that protein aggregates induced by con A-coated beads, some of which are quite large, diffuse almost as fast as single membrane proteins. A trivial explanation for these results would be that a con A-coated bead binds to only one or a few membrane glycoproteins independent of its size. This, however, is unlikely. Measurements of protein adsorption on colloidal gold particles predict that the number of proteins bound depends on the size of the protein and the size of the particle in a predictable manner (De Roe et al., 1987). According to this analysis, our smallest particles, 40 nm, should bind ~240 con A molecules. Particles carrying so many multivalent ligands should form many links to membrane proteins, providing that the membrane proteins are relatively
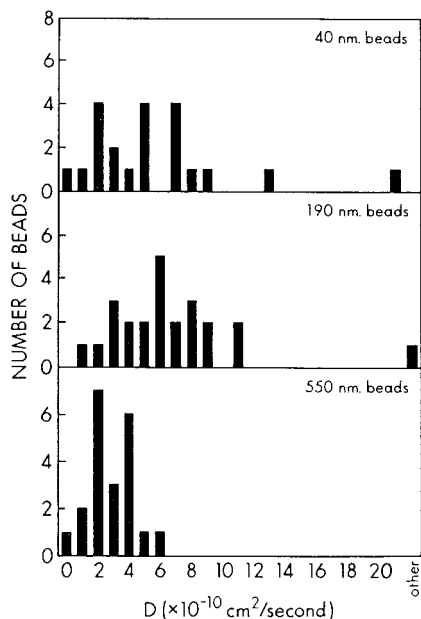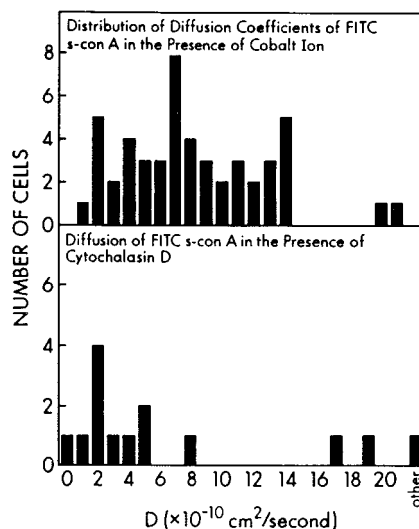

FIGURE 3   Distribution of diffusion coefficients obtained from single particle tracking (SPT) data. While the mean D of the 550-nm beads is significantly different from that of the 40-nm beads and of the FITC-s-con A-labeled membrane proteins (see Table 1), the difference is small (less than a factor of 2) This small difference is inconsistent with transient binding and corral models and supports a hydrodynamic model of retardation of diffusion (see Discussion).

TABLE 1   Summary of all FRAP and SPT measurements

Treatment	Technique	Diffusing Species	D ($\pm$s.d.) $\times$ 10^{-10}
Cyto D	FRAP	FITC s-con A	7.2 $\pm$ 2.8
$CoCl_2$	FRAP	FITC s-con A	8.6 $\pm$ 4.6
None	SPT	40-nm bead	6.1 $\pm$ 4.6
None	SPT	190-nm bead	7.2 $\pm$ 4.9
None	SPT	550-nm bead	3.1 $\pm$ 1.4

abundant. To establish directly that our largest beads were forming protein aggregates, we examined the contact area between the 500-nm beads and the cell surface by electron microscopy. As shown in Fig. 5, the large beads form extensive areas of contact with the membrane.

The size of a membrane protein aggregate formed by such a bead will depend on the contact area of the bead with the membrane. Assuming a constant density of con A molecules per unit area of the microspheres (De Roe et al., 1987), larger beads, with larger contact areas, will form larger membrane protein aggregates. Although we do not have a direct measure of the change in contact area with bead size in this system, it is possible to analyze the functional dependence of contact area on bead diameter. This analysis yields a dependence of contact area on R^2, where R is the radius of the bead. Hence, n, the number of con A molecules linked to a bead, should also vary as R^2. A detailed discussion of this is provided in the Appendix.

The predicted behavior of such bead-induced protein aggregates in random motion in the plane of the membrane is different for the three models of retardation of diffusion that we considered. We interpret these results in terms of various models for retardation of diffusion, as follows.

MODELS FOR MEMBRANE GLYCOPROTEIN DIFFUSION

The microcorral model

According to the microcorral hypothesis, diffusion in the cell membrane is limited by barriers which form restrictive enclosures, or "microcorrals" (Sheetz, 1983). This term is used to distinguish small divisions of the membrane, below the resolution of SPT on a 33-ms time scale, from the larger "confinement zones" (0.25–1.5 μm diam.) which are

readily visible in particle tracks. These barriers might be composed of submembrane filaments that are constantly undergoing rearrangement. In the absence of hydrodynamic effects caused by these immobile structures (Bussell et al., 1995a; Dodd et al., 1995), within a microcorral a membrane protein could move rapidly, at a rate limited only by lipid viscosity. While not directly observable by conventional means, the rate of diffusion within microcorrals could then be as high as that measured for proteins in artificial lipid bilayers at 25°C, $\sim 2 \times 10^{-8}$ cm^2/s (Tank et al., 1982). To diffuse over distances greater than the dimensions of the microcorral, however, a barrier would have to be removed to allow the protein to pass into the adjacent microcorral. Although diffusion within microcorrals might be slower than in reconstituted membranes because of hydrodynamic effects from immobile proteins, breakdown of these barriers might still be the dominant influence on lateral mobility of membrane proteins. Therefore, we consider the possibility that very small corrals, which would not be directly observable, i.e., with dimensions on the order of 0.1 μm, might account for the observed slow diffusion (Sheetz, 1983, 1995; Kusumi et al., 1993; Saxton, 1994, 1995). This model would explain retardation of individual proteins, but would predict much more retarded motion for large protein aggregates. In the present studies, aggregates formed by the larger beads would be expected to span across boundaries of several microcorrals. Assuming that these barriers break down independently with a probability P_b, the probability that n barriers would simultaneously disappear is $(P_b)^n$. The number, n, of submembrane barriers interacting with the bead at any moment should be proportional to the area of contact between bead and cell membrane. The rate-limiting step for diffusion would, therefore, depend exponentially on n, which should in turn depend on R^2, i.e., $(P_b)^n \sim (P_b)^{R^2}$.
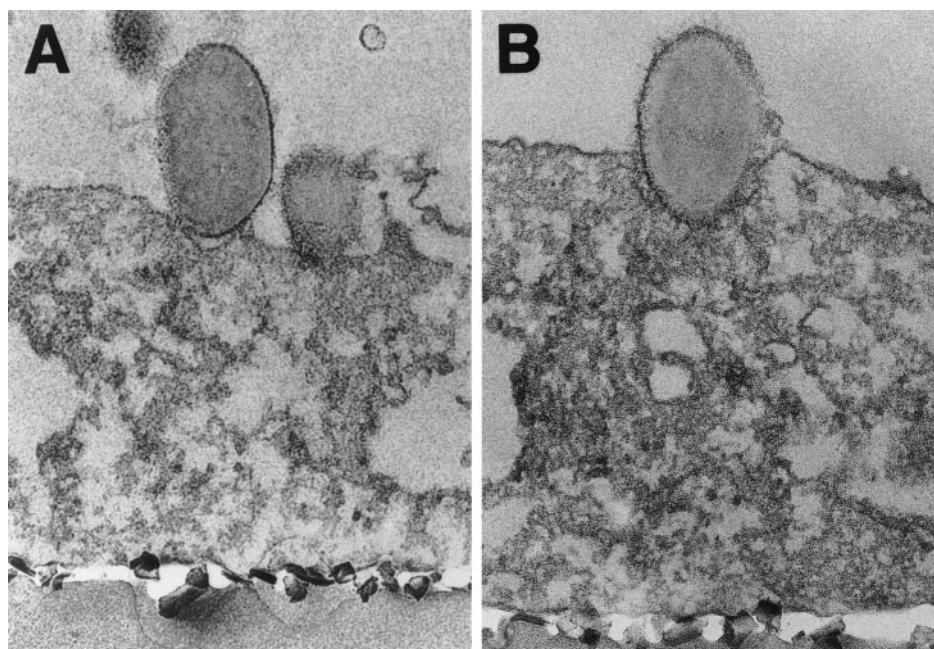

FIGURE 5 Electron microscopy illustrates extensive contact between con A-coated 0.5-μm latex beads and the plasma membrane. While there is a range of contact areas, illustrated by panels (A) and (B), the beads were never seen to be attached at a single point.

The value of R^2 increases 189-fold between the 40- and 550-nm beads. If P_b is not too close to 1, this should be sufficient to rule out the microcorral hypothesis. For example, if $P_b = 0.98$ (a transient barrier that exists only 2% of the time), $(P_b)^{R^2} = 0.02$. A 50-fold change in diffusion rate would have been easily detectable in our measurements, but was not seen. Any value of $P_b < 0.98$ (representing a more substantial barrier) predicts an even stronger dependence of D on aggregate size. Hence the microcorral model is ruled out by our experimental measurements.

Transient binding models

A transient binding model predicts that the diffusion of cell surface proteins is impeded by interactions between the mobile proteins and slowly moving or immobile structures in the cytoplasm, e.g., cytoplasmic proteins bound to the cytoskeleton (cf. Zhang et al., 1991). These interactions could be direct or indirect. An equivalent situation would be transient binding to external structures, e.g., glycosyl moieties on the surface of the cell, or the extracellular matrix. If the lifetime of the bound state were long compared to the time required for measuring diffusion rate, the bound protein would appear immobile. If, however, the lifetime of the bound state were short compared to the measurement time, the protein molecule would bind and detach many times during the measurement. It would, therefore, appear mobile, with its diffusion coefficient reduced by the fraction of the time it spent in the bound state (Elson and Reidler, 1979).

A realistic analysis would allow for independent formation and breakage of bonds within the contact region. If there is a probability P that each membrane protein will be transiently immobilized at any instant, and a probability Q that it will be diffusing freely, then the probability that at least one of a group of n proteins on the surface of a bead will be immobilized at any time is $1 - Q^n$. Although the molecular mechanism is different from that of the microcorral model, i.e., binding versus steric confinement, the consequences for protein aggregates are similar. Assuming a uniform density of con A on the beads, an exponential dependence on n again results in an exponential dependence on R^2. If even one of the proteins attached to the bead is immobilized at any given time, the bead will be immobile. Thus, as the number of con A receptors attached to the bead increases, the probability that the bead will be immobile at any time rapidly approaches 1. A strong dependence of D on bead size is thus predicted, so a transient binding model is inconsistent with our data.

Viscous models

Since we do not know the extent of permeation of lipid molecules into the bead-induced protein aggregates, it is necessary to consider two classes of hydrodynamic models. The consequences for retardation of protein diffusion are different, depending on whether the aggregates behave as impermeable cylinders or are free-draining. We cannot directly measure the density of membrane proteins bound to our beads. We can, however, infer from our data that these proteins are diffusing as unit aggregates, as follows.

Free-draining aggregate diffusion

One might suppose that the patch of membrane glycoproteins linked to the bead is to some extent penetrated by lipid molecules (Wiegel, 1979; Clegg and Vaz, 1985). Let us consider the "free draining" limit in which the membrane glycoproteins experience interactions with the lipid unperturbed by the presence of the other glycoproteins linked to the bead (Flory, 1953). (We would expect that this situation would prevail only if the glycoproteins were sparse and widely spaced.) Then the frictional coefficient of the aggregate is the sum of the frictional coefficients of the individual glycoproteins linked to the bead. In that case, the diffusion coefficient of a bead should be inversely proportional to the number of glycoprotein molecules linked to it. Hence, the diffusion coefficient should vary inversely as R^2 (as should the area of contact; see Appendix). This is a much stronger dependence than is experimentally observed. Therefore, we conclude that aggregates formed by our beads are sufficiently dense to be treated as impermeable cylinders.

Unit aggregate diffusion

A protein aggregate impermeable to lipid molecules and diffusing as a unit in a viscous layer of lipid, surrounded on both sides by aqueous media, has stimulated detailed theoretical analyses. The simplest of these (Saffman and Delbruck, 1975) considers a cylinder of radius R_c and height, h, embedded in a viscous (lipid) layer of thickness h and viscosity μ with both surfaces in contact with a less viscous (aqueous) phase with viscosity μ'. The translational diffusion coefficient of the cylindrical particle in the layer is

$$D = (kT/4\pi\mu h)\log[(\mu h/\mu' R_c) - \gamma] \qquad (4)$$

where γ = Euler's constant. This theory adequately describes the lateral mobility of membrane proteins in reconstituted membranes (at high dilution). If the aggregate of membrane glycoproteins bound to a bead forms an impermeable cylindrical patch, it should diffuse at a rate predicted by this equation (in a system dominated by simple viscous interactions without other retarding influences). The weak dependence of D on R_c predicted by this model is consistent with our experimental observations. The actual value of D, however, would be much greater if we assume unobstructed diffusion of individual membrane protein molecules embedded in a membrane bilayer with a viscosity determined from measurements of lipid diffusion [~2 poise (McCloskey and Poo, 1984)]. A system dominated by simple viscous interactions is consistent with our results, however, only if a much greater effective viscosity is assumed.

If the D observed by us, both by SPT and FRAP (similar to those observed by others in a variety of systems) is used to calculate the effective membrane viscosity of a living cell, then the viscosity limiting the motion of membrane proteins is on the order of 100 poise. This value can be called the "apparent viscosity" of the membrane. Assuming this high apparent viscosity, there would be a very small change in the diffusion coefficient as aggregate size increases. For example, in going from 4 to 200 nm in aggregate radius there would be less than a factor of 2 decrease in diffusion coefficient. This fits very well with our observations.

Excess membrane viscosity beyond that of the lipid bilayer can result from several factors. First, a typical plasma membrane consists of ~50 wt% protein (Alberts et al., 1989). Interactions among the glycoproteins themselves due to their high concentration could substantially diminish their rate of diffusion (Scalettar et al., 1991; Sheetz, 1993). Theory predicts, however, that while this effect is substantial, excluded volume effects alone are insufficient to account for retardation of protein diffusion in cell membranes (Saxton, 1990).

Modern hydrodynamic theory of membrane protein diffusion includes excluded area effects (Saxton, 1990) plus the effects at a distance of both mobile and immobile membrane proteins on a diffusing "tracer" molecule. Among these effects, the drag exerted by immobile particles in an intervening fluid (known as a "fixed bed" in the engineering literature) is especially important. Equations to solve for an effective viscosity based on this "Brinkman screening" were first studied by Brinkman (1947), later fully solved by Howells (1974) and Hinch (1977), and applied to membrane protein diffusion in plasma membranes by Bussell et al. (1995a). This work was extended by Dodd et al. to treat the combined effects of excluded volumes, mobile proteins, and immobile membrane proteins, at higher protein concentrations (Dodd et al., 1995). This theoretical work permits the calculation of an "effective viscosity." This calculation, however, requires that the area fraction of fixed particles is known. In erythrocytes, this has been estimated based on the total area fraction of band 3 (Golan et al., 1984; Saxton, 1990) and its immobile fraction. Since band 3 is by far the predominant membrane protein in erythrocytes, it is reasonable to make a rough approximation based on a single protein species. Most nucleated cells, including the fish epidermal keratocyte, have a much more complex repertoire of membrane proteins, making such estimates unrealistic. Unfortunately, we do not have a way to directly measure the area fraction of immobile (both con A- and non-con-A-binding) proteins in our system. However, all cells have some immobile membrane proteins. Theory predicts that a very small area fraction of fixed proteins (as small as 10^{-5}, according to Bussell et al., 1995b) can exert substantial effects on diffusing proteins. Therefore, it is likely that Brinkman screening contributes to the high apparent viscosity observed in this study.

Interaction with structures exterior to the cell membrane can also contribute to a high apparent viscosity. Steric effects of glycosyl moieties on the surface of the cell or inelastic interactions with the cytoskeleton might also contribute drag. (This is to be distinguished from *transient binding* to the cytoskeleton, which is not consistent with our results.) It is possible that viscous effects both within and exterior to the plasma membrane contribute to the high apparent viscosity observed in our study. This is consistent with experiments measuring diffusion coefficients of membrane protein chimeras by FRAP, which have shown that the apparent diffusion coefficients reflect the sum of the drags from the constituent parts of the protein (Zhang et al., 1991). Although interpreted in terms of a transient binding model, those results are consistent with a viscous hydrodynamic model as well, since size dependence was not tested.

While we cannot determine whether the source of the observed high apparent viscosity is from interactions with structures external to the membrane (i.e., glycosyl moieties on the external surface, or cytoplasmic proteins inside the cell), effects of other proteins embedded in the membrane, or a combination of both, a hydrodynamic model predicts our observations well, while the microcorral and transient binding models do not fit the data.

APPENDIX

In general, the extent of interaction between a con A-coated bead and the cell membrane is governed by the balance between the free energy of interaction of the con A molecules with their membrane glycoprotein binding sites and the free energy of deformation of the cell surface. Evans and Buxbaum (1981) have analyzed this balance in a study of particle encapsulation by erythrocytes. For particles of the size used by Evans and Buxbaum (~1 μm) it is appropriate to assume that the deformability of the erythrocyte membrane is dominated by resistance to shear and that resistance to bending is negligible. We begin by also assuming that in FEKs bending resistance is negligible compared to shear resistance. With this assumption, the fraction of the particle encapsulated depends on g/μ, the ratio of the surface affinity, g (i.e., the free energy reduction per unit area of adhesive contact formed), to the membrane elastic shear modulus, μ, but not explicitly on the radius of the particle. Because the number of con A molecules per unit area of bead surface should also be independent of the size of the bead, the ratio g/μ and, therefore, also the fractional extent of bead encapsulation should be independent of bead size. This can be expressed as

$$A_c/4\pi R^2 = K(g/\mu), \qquad (5)$$

where A_c is the area of contact, R is the radius of the bead, and the function $K(g/\mu)$ is independent of the size of the bead and is given implicitly in Eq. 7 of Evans and Buxbaum (1981) (neglecting terms which depend on the total membrane area). Under these conditions, therefore, $A_c/4\pi R^2$ is a constant for a given value of g/μ, and so $A_c \sim R^2$. Thus, the experimental dependence of diffusion coefficient on bead size can be compared to the predictions of various models for membrane glycoprotein diffusion using this relationship between bead radius and contact area. Also, because the number of membrane glycoproteins bound to the bead is proportional to the area of contact, then that number should also depend on R^2.

Because of the small size of the particles used in our measurements, it might be argued that neglect of bending resistance is less appropriate for our measurements than those of Evans and Buxbaum. As shown by Evans and Buxbaum, there is a threshold condition set by R, g/μ, and B_0, the bending modulus of the membrane, which determines whether the surface affinity is sufficient to drive some deformation of the membrane around the bead. If, on the FEK, the membrane resistance to bending is stabilized, e.g., by cytoskeletal connections, its resistance to bending might be greater than that of the erythrocyte. Our electron microscopic measurements demon-

strate, however, that the largest beads (0.5 μm) were partially encapsulated (Fig. 5). Since we do not know the bending resistance of the FEK membrane, we cannot argue on theoretical grounds that the smallest beads (40-nm) also had many bonds to membrane proteins. Even if one were to assume that the smaller particles were only attached to a single membrane protein, however, it would only strengthen our conclusions regarding the models of membrane protein diffusion, since the dependence of aggregate size on bead size would be even greater than we have assumed.

REFERENCES

Alberts, B., D. Bray, J. Lewis, M. Raff, K. Roberts, and J. D. Watson. 1989. The Plasma Membrane. *In* Molecular Biology of the Cell. B. Alberts, D. Bray, J. Lewis, M. Raff, K. Roberts, and J. D. Watson, editors. Garland Publishing, Inc., New York, NY. 276–341.

Axelrod, D., D. E. Koppel, J. Schlessinger, E. Elson, and W. W. Webb. 1976. Mobility measurement by analysis of fluorescence photobleaching recovery kinetics. *Biophys. J.* 16:1055–1069.

Brinkman, H. C. 1947. A calculation of the viscous force exerted by a flowing liquid on a dense swarm of particles. *Appl. Sci. Res. A.* 1:27–34.

Bussell, S. J., D. L. Koch, and D. A. Hammer. 1995a. Effect of hydrodynamic interactions on the diffusion of integral membrane proteins: diffusion in plasma membranes. *Biophys. J.* 68:1836–1849.

Bussell, S. J., D. L. Koch, and D. A. Hammer. 1995b. Effect of hydrodynamic interactions on the diffusion of integral membrane proteins: tracer diffusion in organelle and reconstituted membranes. *Biophys. J.* 68: 1828–1835.

Clegg, R. M., and W. L. C. Vaz. 1985. Translational diffusion of proteins and lipids in artificial lipid bilayer membranes. A comparison of experiment with theory. *In* Progress in Protein-Lipid Interactions. A. Watts and J. H. M. de Pont, editors. Elsevier, Amsterdam. 173–229.

Cooper, M. S., and M. Schliwa. 1986. Motility of cultured fish epidermal cells in the presence and absence of direct current electric fields. *J. Cell Biol.* 102:1384–1399.

de Brabander, M., R. Nuydens, A. Ishihara, B. Holifield, K. Jacobson, and H. Geerts. 1991. Lateral diffusion and retrograde movements of individual cell surface components on single motile cells observed with Nanovid microscopy. *J. Cell Biol.* 112:111–124.

De Roe, C., P. J. Courtoy, and P. Baudhuin. 1987. A model of protein-colloidal gold interactions. *J. Histochem. Cytochem.* 35:1191–1198.

Dodd, T. L., D. A. Hammer, A. S. Sangani, and D. L. Koch. 1995. Numerical simulations of the effect of hydrodynamic interactions on diffusivities of integral membrane proteins. *J. Fluid Mech.* 293:147–180.

Dubinsky, J. M., D. J. Loftus, G. D. Fischbach, and E. L. Elson. 1989. Formation of acetylcholine receptor clusters in chick myotubes: migration or new insertion? *J. Cell Biol.* 109:1733–1743.

Elson, E. L., and J. A. Reidler. 1979. Analysis of cell surface interactions by measurements of lateral mobility. *J. Supramol. Struct.* 12:481–489.

Evans, E., and K. Buxbaum. 1981. Affinity of red blood cell membrane for particle surfaces measured by the extent of particle encapsulation. *Biophys. J.* 34:1–12.

Flory, P. J. 1953. Principles of Polymer Chemistry. Cornell University Press, Ithaca, NY. 1 p.

Gelles, J., B. J. Schnapp, and M. P. Sheetz. 1988. Tracking kinesin-driven movements with nanometre-scale precision. *Nature.* 331:450–453.

Golan, D. E., M. R. Alecio, W. R. Veatch, and R. R. Rando. 1984. Lateral mobility of phospholipid and cholesterol in the human erythrocyte membrane: effects of protein-lipid interactions. *Biochemistry.* 23: 332–339.

Golan, D. E., J. D. Corbett, C. Korsgren, H. S. Thatte, S. Hayette, Y. Yawata, and C. M. Cohen. 1996. Control of band 3 lateral and rotational mobility by band 4.2 in intact erythrocytes: release of band 3 oligomers from low-affinity binding sites. *Biophys. J.* 70:1534–1542.

Hinch, E. J. 1977. An averaged-equation approach to particle interactions in a fluid suspension. *J. Fluid Mech.* 83:695–720.

Howells, I. D. 1974. Drag due to the motion of a Newtonian fluid through a sparse random array of small fixed objects. *J. Fluid Mech.* 64: 449–475.

Jacobson, K., A. Ishihara, and R. Inman. 1987. Lateral diffusion of proteins in membranes. *Annu. Rev. Physiol.* 49:163–175.

Kolega, J. 1986. Effects of mechanical tension on protrusive activity and microfilament and intermediate filament organization in an epidermal epithelium moving in culture. *J. Cell Biol.* 102:1400–1411.

Kucik, D. F., E. L. Elson, and M. P. Sheetz. 1989. Forward transport of glycoproteins on leading lamellipodia in locomoting cells. *Nature.* 340: 315–317.

Kucik, D. F., E. L. Elson, and M. P. Sheetz. 1990. Cell migration does not produce membrane flow. *J. Cell Biol.* 111:1617–1622.

Kucik, D. F., S. C. Kuo, E. L. Elson, and M. P. Sheetz. 1991. Preferential attachment of membrane glycoproteins to the cytoskeleton at the leading edge of lamella. *J. Cell Biol.* 114:1029–1036.

Kusumi, A., Y. Sako, and M. Yamamoto. 1993. Confined lateral diffusion of membrane receptors as studied by single particle tracking (nanovid microscopy). Effects of calcium-induced differentiation in cultured epithelial cells. *Biophys. J.* 65:2021–2040.

Martenson, C., K. Stone, M. Reedy, and M. Sheetz. 1993. Fast axonal transport is required for growth cone advance. *Nature.* 366:66–69.

McCloskey, M., and M. M. Poo. 1984. Protein diffusion in cell membranes: some biological implications. *Int. Rev. Cytol.* 87:19–81.

Qian, H., M. P. Sheetz, and E. L. Elson. 1991. Single particle tracking. Analysis of diffusion and flow in two-dimensional systems. *Biophys. J.* 60:910–921.

Saffman, P. G., and M. Delbruck. 1975. Brownian motion in biological membranes. *Proc. Natl. Acad. Sci. USA.* 72:3111–3113.

Sako, Y., and A. Kusumi. 1995. Barriers for lateral diffusion of transferrin receptor in the plasma membrane as characterized by receptor dragging by laser tweezers: fence versus tether. *J. Cell Biol.* 129:1559–1574.

Saxton, M. J. 1990. Lateral diffusion in a mixture of mobile and immobile particles. A Monte Carlo study. *Biophys. J.* 58:1303–1306.

Saxton, M. J. 1994. Single-particle tracking: models of directed transport. *Biophys. J.* 67:2110–2119.

Saxton, M. J. 1995. Single-particle tracking: effects of corrals. *Biophys. J.* 69:389–398.

Saxton, M. J., and K. Jacobson. 1997. Single particle tracking—applications to membrane dynamics. *Annu. Rev. Biophys. Biomolec. Struct.* 26:373–399.

Scalettar, B. A., J. R. Abney, and C. R. Hackenbrock. 1991. Dynamics, structure, and function are coupled in the mitochondrial matrix. *Proc. Natl. Acad. Sci. U.S.A.* 88:8057–8061.

Sheetz, M. P. 1983. Membrane skeletal dynamics: role in modulation of red cell deformability, mobility of transmembrane proteins, and shape. *Semin. Hematol.* 20:175–188.

Sheetz, M. P. 1993. Glycoprotein motility and dynamic domains in fluid plasma membranes. *Annu. Rev. Biophys. Biomol. Struct.* 22:417–431.

Sheetz, M. P. 1995. Cellular plasma membrane domains. *Mol. Membr. Biol.* 12:89–91.

Sheetz, M. P., S. Turney, H. Qian, and E. L. Elson. 1989. Nanometre-level analysis demonstrates that lipid flow does not drive membrane glycoprotein movements. *Nature.* 340:284–288.

Svitkina, T. M., A. B. Verkhovsky, K. M. McQuade, and G. G. Borisy. 1997. Analysis of the actin-myosin II system in fish epidermal keratocytes: mechanism of cell body translocation. *J. Cell Biol.* 139: 397–415.

Tank, D. W., E. S. Wu, P. R. Meers, and W. W. Webb. 1982. Lateral diffusion of gramicidin C in phospholipid multibilayers. Effects of cholesterol and high gramicidin concentration. *Biophys. J.* 40:129–135.

Wiegel, F. W. 1979. Hydrodynamics of a permeable patch in the fluid membrane. *J. Theor. Biol.* 77:189–193.

Zhang, F., B. Crise, B. Su, Y. Hou, J. K. Rose, A. Bothwell, and K. Jacobson. 1991. Lateral diffusion of membrane-spanning and glycosylphosphatidylinositol-linked proteins: toward establishing rules governing the lateral mobility of membrane proteins. *J. Cell Biol.* 115: 75–84.